

Energy Research and Development Division
FINAL PROJECT REPORT

Solar-Reflective “Cool” Walls: Benefits, Technologies, and Implementation

Appendix B: Effect of Neighboring Cool Walls on Heating, Ventilation, and Air Conditioning Loads (Task 2.2 Report)

California Energy Commission
Gavin Newsom, Governor

April 2019 | CEC-500-2019-040-APB



Appendix B: Effect of neighboring cool walls on HVAC loads (Task 2.2 report)

Weilong Zhang¹, Matteo Pizzicotti¹, Ronnen Levinson², Nathalie Dumas¹, Benjamin Kurtz¹, Yan Long¹, Negin Nazarian¹, Jan Kleissl¹

¹ Center for Energy Research, University of California, San Diego

² Heat Island Group, Lawrence Berkeley National Laboratory

28 February 2018

Abstract

High albedo (“cool”) walls are exterior building walls with surface (usually paint) properties that increase reflection of solar radiation. Consider a central building with neighbors. Raising the albedo of neighboring walls can increase reflection of downwelling sunlight from neighboring walls to the walls and windows of the central building. The indoor and outdoor building thermal environments in a three-dimensional urban area with a 5×5 array of identical buildings about 23 m apart are simulated. Building energy use effects of cool walls are quantified for a pre-1978 apartment building in Fullerton, CA (Orange County; California climate zone 8).

Daytime heating loads are near zero and changing wall albedo therefore does not modify the daytime heating load. Nighttime cooling loads are small and changing wall albedo therefore mostly influences the daytime cooling load. Raising the neighboring wall albedo increases annual cooling load of the central building by 1.2 MWh (1.2 percent) due to increased solar radiation reflected from the neighboring buildings towards the central building. The cooling load increase for the central building upon raising the albedo of all neighboring walls (1.2 MWh or 1.2 percent) is smaller than the cooling load decrease for the central building upon raising the albedo of its own walls (5.0 MWh, or 5.0 percent). The combined cool wall effect on all buildings is net positive.

Using retroreflective cool walls (albedo 0.60) on all neighboring buildings lowers the annual cooling load of the central building by 3.3 MWh (4.0 percent) with respect to using Lambertian cool walls (also albedo 0.60) on all neighboring buildings. However,

the cooling benefit comes at the expense of a 0.9 MWh (2.6 percent) increase in annual heating load. The net effect of changing to a retroreflective wall from a Lambertian wall on the central building is a reduction in average solar radiation incident on walls, which decreases cooling loads and increases heating loads.

1 Introduction

Global energy consumption increased considerably in the last 20 years and the U.S. Energy Information Administration's projections show a continuing upward trend into the future (EIA, 2017). For residential buildings in California and the U.S., 30 percent and 47 percent, respectively, of the total energy consumed is related to heating, ventilation, and air conditioning, or HVAC (EIA, 2009). HVAC is on average the largest energy expense (EIA, 2009).

Increasing the albedo (solar reflectance) of roof or wall surfaces can cool the building envelope by reducing its solar heat gain. This decreases conduction of heat from the envelope to the building's conditioned space on a warm, sunny day, reducing the need for air conditioning. It also lessens convection of heat from the envelope to city air, mitigating the urban heat island effect (UHIE), or elevation of urban air temperature above that in surrounding rural areas. Cooling the outside air further decreases the air conditioning demand.

Reflective (cool) roofs are a common example of cool urban surfaces and are already prescribed by building energy standards in California and other U.S. states (Akbari and Levinson, 2010; CRRC, 2017). Little of the sunlight reflected by a roof will strike neighboring buildings unless the surrounding buildings are substantially taller. This allows cool roof effects to be evaluated by considering a single building in isolation. Cool urban surfaces other than roofs, such as high-albedo walls and pavements, will reflect sunlight to other elements of the city, including neighboring walls, neighboring windows, and pedestrians.

Yaghoobian et al. (2012) examined such effects on building energy use of cool pavements in an urban canyon using the Temperature of Urban Facets - Indoor Outdoor Building Energy Simulator (TUF-IOBES). Annual heating and cooling loads (quantities of heat added to or removed from the conditioned space to regulate indoor temperature) were simulated for pre-1980 and 1990s office buildings with window-to-wall ratio (net glazed area / gross wall area) 0.47, canyon aspect ratio (building height divided by inter-building separation) 0.37 - 1.5, and pavement albedo 0.10 - 0.50. As expected, they found reduced pavement temperature that led to a lower canopy air temperature. On the other hand, reflecting more sunlight from the pavement heated the walls of adjacent buildings, and increased solar radiation incident on and through windows. This raised summer cooling loads and lowered winter heating loads. Depending on building type and canyon aspect ratio, annual cooling loads increased by 2.2 - 8.3 kWh per square

meter of building floor area for every 0.10 increase in pavement albedo. The overall effect for Phoenix, Arizona was an increase in annual building energy use. However, in Yaghoobian et al. (2012) the effects of cool pavements on daylighting and lighting energy use were neglected.

Cool walls also increase heat transfer between urban surfaces. Consider a central building with neighbors. Raising the albedo of neighboring walls can increase reflection of downwelling sunlight from neighboring walls to the walls and windows of the central building. Raising the albedo of walls on the central building, on neighboring buildings, or on both can increase reflection of sunlight from the central building to neighboring buildings back to the central building. Either mechanism can increase cooling load, decrease heating load, and reduce need for artificial lighting in the central building. Raising central or neighboring building wall albedo also lowers the solar absorptance of the urban canyon, cooling the air within.

The Center for Energy Research at the University of California, San Diego (UCSD) partnered with Lawrence Berkeley National Laboratory (LBNL) to quantify the effect of cool walls on building energy use. The current report extends the analysis in the Task 2.1 report: *Simulated HVAC energy savings in an isolated building* to account for building-to-building interactions on building heating and cooling loads. It considers both diffusely reflecting walls and retroreflective walls. Building-to-building interaction on lighting loads will be analyzed in future work.

The report is structured as follows. Section 2 (Theory) contains a theoretical analysis of radiative interaction within an array of buildings. Section 3 (Methodology) starts with a description of the computer model in Section 3.1. Section 3.2 describes how we calculate the effect on the thermal load of a central building of changing the albedo of neighboring walls, in the common case where all walls reflect diffusely. Section 3.3 presents a variation in which the walls are retroreflective. Section 3.4 details the simulation setup, including weather, building thermal properties, and building equipment. Section 4 (Results and Discussion) contains the outcomes, and the take-away is provided in Section 5 (Conclusions).

2 Theory

Here we assess how reflection from the walls of neighboring buildings contributes to the wall solar heat gain of a central building. We also consider how that solar heat gain is affected by changes in the albedos of walls on the central building and on the neighboring buildings.

The buildings are assumed to be rectangular, cardinally oriented, and regularly spaced. In the first scenario, the buildings are square, with equal north-south and east-west

separations. The second scenario relaxes the requirements of the first scenario, but orients half the buildings with long axis north-south, and half with long axis east-west.

2.1 Central-building wall solar heat gain in regularly spaced array of rectangular buildings

Consider a regularly spaced array of cardinally oriented rectangular buildings—that is, buildings with outer walls facing due north (N), east (E), south (S), and west (W)—with separation δ_{NS} between the N and S walls of adjacent buildings, and separation δ_{EW} between the E and W walls of adjacent buildings. If each wall of the central building (subscript c) sees parallel, but not perpendicular, walls of neighboring buildings (subscript n), the total wall solar heat gain (power) of the central building will be

$$K = (1 - \rho_c) \left[(A_{N,c} I_N + A_{E,c} I_E + A_{S,c} I_S + A_{W,c} I_W) + \rho_n (A_{N,n} I_N F_{N,n \rightarrow S,c} + A_{E,n} I_E F_{E,n \rightarrow W,c} + A_{S,n} I_S F_{S,n \rightarrow N,c} + A_{W,n} I_W F_{W,n \rightarrow E,c}) \right] \quad (1)$$

where ρ is wall albedo; A is wall area; I is wall irradiance (power/area), assumed spatially uniform; and $F_{X \rightarrow Y}$ is the view factor from surface X to surface Y . Here subscript “ D,c ” denotes the central building wall facing direction D , while the subscript “ D,n ” refers to the multi-element surface comprising all neighboring walls that face direction D and see the central building. The first term in the bracket sums downwelling incident solar radiation, while the second term sums diffuse reflection to the central walls of downwelling sunlight incident on the neighboring walls.¹ Applying the view factor reciprocity relationship

$$A_X F_{X \rightarrow Y} = A_Y F_{Y \rightarrow X} \quad (2)$$

and rearranging,

$$K = (1 - \rho_c) \left[A_N I_N (1 + \rho_n F_{N,c \rightarrow S,n}) + A_E I_E (1 + \rho_n F_{E,c \rightarrow W,n}) + A_S I_S (1 + \rho_n F_{S,c \rightarrow N,n}) + A_W I_W (1 + \rho_n F_{W,c \rightarrow E,n}) \right] \quad (3)$$

¹ Light reflected from central building to neighboring walls and back to the central building is neglected; the ratio of this flux to that in the second term of Eq. (1) would be equal to $\rho_c F_{D,c \rightarrow D,n}$, which tends to be small (typically < 20 percent). If, say, $F_{D,c \rightarrow D,n} = 0.13$ as for the multifamily building array in this report, the ratio will be 3.3 percent for a conventional central wall ($\rho_c = 0.25$) or 7.8 percent for a cool central wall ($\rho_c = 0.60$).

2.2 Scenario 1: Evenly spaced array of square buildings

If the buildings are square and have equal N-S and E-W spacings, the total wall solar heat gain can be expressed as

$$K_0 = (1 - \rho_c) (I_N + I_E + I_S + I_W) A_0 (1 + F_0 \rho_n), \quad (4)$$

where A_0 is the area of each wall and F_0 is the view factor from each central wall to the extended surface comprised of all parallel neighboring walls. F_0 is most sensitive to the distance $\delta_{NS} = \delta_{EW}$ between the central wall and the neighboring wall. Since the adjacent wall dominates the view factor towards all walls, the view factor to all walls decreases approximately as δ_{NS}^2 following the Nusselt analog for view factors².

Raising the albedo of neighboring walls by $\Delta\rho_n$ will increase the central building's total wall solar heat gain by

$$\Delta K_0 = (1 - \rho_c) (I_N + I_E + I_S + I_W) A_0 F_0 \Delta\rho_n. \quad (5)$$

Using view factor reciprocity [Eq. (2)], we can also express this increase in terms of the area A_n of the extended surface comprised of all parallel neighboring walls, and the view factor F_n from this surface to the central wall:

$$\Delta K_0 = (1 - \rho_c) (I_N + I_E + I_S + I_W) A_n F_n \Delta\rho_n. \quad (6)$$

This alternative formulation shows that the increase in the central building's total wall solar heat gain is proportional to the area A_n of the modified neighboring wall.

Returning to the original formulation, the fractional increase in K will be

$$f_{K_0} \equiv \frac{\Delta K_0}{K_0} = \frac{F_0 \Delta\rho_n}{1 + F_0 \rho_n}. \quad (7)$$

where ρ_n is the initial (pre-raise) albedo of the neighboring wall. We can compare the absolute increase in K_0 on raising the albedo of neighboring walls to the absolute *decrease* in K_0 upon raising the albedo of the central building walls. The ratio of the former to the latter will be

² Nusselt (1928) proposed to calculate view factors as the conical projection of the receiving surface on a unit sphere around the emitting surface. The view factor from the emitting surface to the receiving surface is then the fraction of the circle occupied by the conical projection.

$$g \equiv \frac{(1 - \rho_c) (I_N + I_E + I_S + I_W) A_0 F_0 \Delta\rho_n}{(I_N + I_E + I_S + I_W) A_0 (1 + F_0 \rho_n) \Delta\rho_c} = \frac{F_0 (1 - \rho_c) \Delta\rho_n}{(1 + F_0 \rho_n) \Delta\rho_c}. \quad (8)$$

where ρ_c is the initial (pre-raise) albedo of the central wall. If $\Delta\rho_n = \Delta\rho_c$,

$$g = \frac{F_0 (1 - \rho_c)}{1 + F_0 \rho_n}. \quad (9)$$

2.3 Scenario 2: Half the buildings oriented N-S, half oriented E-W

We relax the requirements of the first scenario, but divide the buildings into two side-by-side sets of equal population, each set contiguous. In set A, where streets run N-S, the long axis of each building extends N-S, making the E and W walls longer than the N and S walls. The buildings in set B, where streets run E-W, are rotated 90° from those in set A, with the long axis extending E-W, and the N and S walls longer than the E and W walls. Differences in building-to-building shading may cause wall irradiances to vary by set.

Let A_1 and A_2 represent the area of each long wall and each short wall, respectively, and F_1 and F_2 represent the view factors from each central long wall to its parallel neighboring walls and from each central short wall to its parallel neighboring walls, respectively. In set A, $A_E = A_W = A_1$, $A_N = A_S = A_2$, $F_{E,c \rightarrow W,n} = F_{W,c \rightarrow E,n} = F_1$, and $F_{N,c \rightarrow S,n} = F_{S,c \rightarrow N,n} = F_2$. In set B, $A_N = A_S = A_1$, $A_E = A_W = A_2$, $F_{N,c \rightarrow S,n} = F_{S,c \rightarrow N,n} = F_1$, and $F_{E,c \rightarrow W,n} = F_{W,c \rightarrow E,n} = F_2$. Hence for a central building in set A,

$$K_A = (1 - \rho_c) [A_1 (1 + \rho_n F_1) (I_{E,A} + I_{W,A}) + A_2 (1 + \rho_n F_2) (I_{N,A} + I_{S,A})], \quad (10)$$

and for a central building in set B,

$$K_B = (1 - \rho_c) [A_1 (1 + \rho_n F_1) (I_{N,B} + I_{S,B}) + A_2 (1 + \rho_n F_2) (I_{E,B} + I_{W,B})]. \quad (11)$$

Averaging over the two sets yields the population average total wall solar heat gain

$$\bar{K} \equiv \frac{K_A + K_B}{2} = \frac{(1 - \rho_c)}{2} [A_1 (1 + \rho_n F_1) (I_{N,B} + I_{E,A} + I_{S,B} + I_{W,A}) + A_2 (1 + \rho_n F_2) (I_{N,A} + I_{E,B} + I_{S,A} + I_{W,B})]. \quad (12)$$

Raising the albedo of neighboring walls by $\Delta\rho_n$ will increase \bar{K} by

$$\Delta\bar{K} = \frac{(1 - \rho_c)}{2} [A_1 F_1 \Delta\rho_n (I_{N,B} + I_{E,A} + I_{S,B} + I_{W,A}) + A_2 F_2 \Delta\rho_n (I_{N,A} + I_{E,B} + I_{S,A} + I_{W,B})]. \quad (13)$$

The fractional increase in \bar{K} will be

$$f_{\bar{K}} = \frac{\Delta \bar{K}}{\bar{K}} = \frac{A_1 F_1 \Delta \rho_n (I_{N,B} + I_{E,A} + I_{S,B} + I_{W,A}) + A_2 F_2 \Delta \rho_n (I_{N,A} + I_{E,B} + I_{S,A} + I_{W,B})}{A_1 (1 + \rho_n F_1) (I_{N,B} + I_{E,A} + I_{S,B} + I_{W,A}) + A_2 (1 + \rho_n F_2) (I_{N,A} + I_{E,B} + I_{S,A} + I_{W,B})}. \quad (14)$$

where ρ_n is the initial (pre-raise) albedo of the neighboring wall. As before, we can compare the absolute increase in \bar{K} on raising the albedo of neighboring walls to the *decrease* in \bar{K} upon raising the albedo of the central building walls. The ratio of the former to the latter will be

$$g = \frac{\frac{(1-\rho_c)}{2} [A_1 F_1 \Delta \rho_n (I_{N,B} + I_{E,A} + I_{S,B} + I_{W,A}) + A_2 F_2 \Delta \rho_n (I_{N,A} + I_{E,B} + I_{S,A} + I_{W,B})]}{\frac{1}{2} [A_1 (1 + \rho_n F_1) (I_{N,B} + I_{E,A} + I_{S,B} + I_{W,A}) + A_2 (1 + \rho_n F_2) (I_{N,A} + I_{E,B} + I_{S,A} + I_{W,B})] \Delta \rho_c}. \quad (15)$$

where ρ_c is the initial (pre-raise) albedo of the central wall. In the special case in which neighboring walls on the same side of the street are close enough to keep each other in shadow and to have small view factors to the sky, $I_{N,A} = I_{E,B} = I_{S,A} = I_{W,B} \approx 0$. Then

$$f_{\bar{K}} \equiv \frac{\Delta \bar{K}}{\bar{K}} = \frac{A_1 F_1 \Delta \rho_n (I_{N,B} + I_{E,A} + I_{S,B} + I_{W,A})}{A_1 (1 + \rho_n F_1) (I_{N,B} + I_{E,A} + I_{S,B} + I_{W,A})} = \frac{F_1 \Delta \rho_n}{(1 + F_1 \rho_n)} \quad (16)$$

and

$$g = \frac{\frac{(1-\rho_c)}{2} [A_1 F_1 \Delta \rho_n (I_{N,B} + I_{E,A} + I_{S,B} + I_{W,A})]}{\frac{1}{2} [A_1 (1 + \rho_n F_1) (I_{N,B} + I_{E,A} + I_{S,B} + I_{W,A})] \Delta \rho_c} = \frac{F_1 \Delta \rho_n (1 - \rho_c)}{(1 + F_1 \rho_n) \Delta \rho_c}. \quad (17)$$

If $\Delta \rho_n = \Delta \rho_c$,

$$g = \frac{F_1 (1 - \rho_c)}{1 + F_1 \rho_n}. \quad (18)$$

Note how $f_{\bar{K}}$ and g take the same form as in Scenario 1, changing only the view factor to F_1 from F_0 .

3 Simulation methodology

3.1 Temperature of Urban Facets Indoor – Outdoor Building Energy Simulator

The simulations in this chapter employ the TUF-IOBES model that simulates indoor and outdoor building surface and air temperatures and heat fluxes in a three-dimensional urban area with a 5×5 array of identical buildings. The indoor and outdoor energy balances are dynamically coupled and forced by outdoor weather conditions, building envelope properties, urban material properties, indoor heat sources, and HVAC systems (Figure 1).

Any (indoor or outdoor) surface energy balance can include shortwave (SW) and longwave (LW) radiation, conduction, convection of sensible and latent heat, and phase change. Beam (a.k.a. direct) and diffuse solar radiation and downwelling longwave radiation from the sky, as well as sunlight reflected by and LW radiation emitted by the ground and neighboring buildings, are partly absorbed by exterior wall and roof surfaces. This heat is then transferred through the wall or roof via conduction, to the outside air via convection, or to the surroundings via longwave radiation. Windows also admit sunlight.

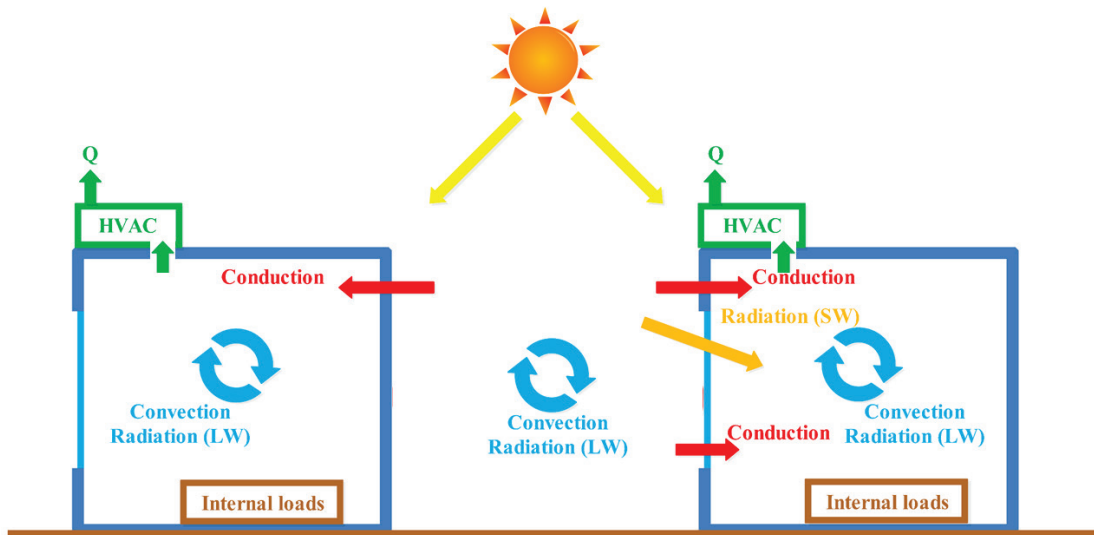


Figure 1. Illustration of the heat transfer process in the TUF-IOBES building-to-canopy model during the cooling season. Q is heat exhaust from the HVAC. TUF-IOBES simulates a 3D domain with an array of 5 × 5 buildings, but here only a cross section through two buildings is shown.

The interior wall or ceiling surface energy balance includes conduction through the building envelope, convection to the room air, absorption of shortwave radiation, and longwave radiation exchange between indoor surfaces. Shortwave (solar spectrum) radiation comes from windows and lamps, while longwave (thermal infrared) radiation emits from interior envelope surfaces, equipment, and occupants.

The outdoor energy balance yields the canopy air and urban surface temperatures and is forced by weather data. In turn, outdoor conditions affect the indoor environment. The internal surface temperatures, indoor air temperature, and building thermal loads are obtained from the indoor energy balance model. If the indoor air temperature is outside the setpoint range, thermal energy (heat) is added or removed to bring the temperature within the setpoint range; this thermal energy constitutes the heating or cooling load. The air-conditioning (AC) system transfers the cooling load waste heat from the indoor to the outdoor environment, increasing the canopy air temperature. Heating equipment

is assumed to be electric resistance and all heat produced by the heating equipment increases interior air temperature; i.e. the heating equipment does not exhaust waste heat to the outside air. The TUF-IOBES model has been described and validated in detail by Yaghoobian and Kleissl (2012).

3.2 Effects of raising neighboring building wall albedo on the heat balance of the central building

Raising the albedo of walls on neighboring buildings affects the heat balance of the central building. A cool (high albedo) wall of a neighboring building increases shortwave irradiance and decreases longwave irradiance on the opposing wall of the central building compared to the case with conventional (lower albedo) walls on the neighboring building. The widespread use of cool walls may also reduce canyon air temperature. However, this effect is expected to be minor if only a few buildings are assigned cool walls, and is neglected here.³

The TUF-3D radiation model in TUF-IOBES uses periodic boundary conditions on a single building (the central building unit, or CBU) to simulate a 5×5 array of buildings.⁴ This setup does not allow wall albedo to vary building to building. Therefore, a workaround was devised to examine the effect of neighboring buildings with cool walls on a CBU with conventional walls, or that of neighboring buildings with conventional walls on a CBU with cool walls. The following cases are simulated for the 5×5 array of buildings:

- C25N25: All central (“C”) and neighboring (“N”) building walls are conventional (albedo 0.25). Note the use of “N” to mean “neighboring”, rather than “north”, in the case labels.
- C60N60: All central and neighboring building walls are cool (albedo 0.60).
- C25N60: All central and neighboring building walls are conventional (albedo 0.25), but shortwave and longwave irradiances on every wall of the CBU are assigned values consistent with facing a cool neighboring wall of albedo 0.60. That is, irradiances on CBU walls are taken from the C60N60 simulation.

³ The Task 3.2 report: *Urban climate impacts of cool walls* assesses canyon air temperature reduction upon raising wall albedo.

⁴ The TUF-3D solver imitates periodic boundary conditions by solving for reflected radiances only for patches in the central urban unit, and setting radiative and energy balance exchanges of all other patches equal to those of the corresponding patch within the central urban unit (Krayenhoff and Voogt, 2007).

- C60N25: All central and neighboring building walls are cool (albedo 0.60), but shortwave and longwave irradiances on every wall of the CBU are assigned values consistent with facing a conventional neighboring wall of albedo 0.25. That is, irradiances on CBU walls are taken from the C25N25 simulation.

We can use these load profiles to evaluate four albedo-change scenarios:

- a) raising the albedo of all central walls, leaving all neighboring walls conventional (C60N25 - C25N25);
- b) raising the albedo of all neighboring walls when all central walls remain conventional (C25N60 - C25N25);
- c) raising the albedo of all neighboring walls when all central walls are cool (C60N60 - C60N25); and
- d) raising the albedo of all central walls and all neighboring walls (C60N60 - C25N25).

The workaround incorporates the following assumptions:

- i. The component of central wall irradiance due to reflection from central wall to opposing neighboring wall back to central wall is small. This is reasonable if the wall-to-wall view factor F_0 (the view factor from each central wall to the extended surface comprised of all parallel neighboring walls) is modest, because the wall-to-walls-to-wall reflection would be proportional to the square of this view factor. For example, if $F_0 = 0.13$, then F^2 is 0.017. This wall-to-walls-to-wall radiation is further diminished by absorption at the neighboring walls.
- ii. Spatial variations in wall irradiance (that is, variations across the face of a given wall) induced by partial shading are neglected. The average shortwave and longwave irradiances across each wall are input to the heterogeneous simulations. Intra-wall differences are expected to be small except when parts of the wall are shaded by surrounding buildings shortly after sunrise or shortly before sunset.

3.3 Retroreflector analysis

In this section, the methodology for studying the effect of retroreflective (RR) walls on building energy use is presented. Retroreflective cool walls improve upon diffusely reflecting cool walls by reflecting incoming beam radiation toward the solar disc (if a retroreflection is three dimensional) or at least upwards (if the retroreflection is two dimensional). This can increase the fraction of sunlight reflected out of the urban canyon.

Depending on the canyon aspect ratio, a large fraction of the sunlight reflected by diffusely reflecting cool walls could remain trapped between buildings due to reflection towards ground or neighboring wall surfaces with low albedo. For example, consider an isolated building with 0.60 wall albedo and 0.10 ground albedo, each surface a perfectly diffuse reflector. About 33 percent of the sunlight incident on the wall would return to the sky [$0.60 \text{ wall albedo} \times (0.5 \text{ sky view factor} + 0.5 \text{ ground view factor} \times 0.10 \text{ ground albedo})$]. If the wall were instead covered with a 2D retroreflector (pairs of orthogonal surfaces, each of albedo 0.775, with a two-bounce albedo of $0.775^2 = 0.60$), it would reflect upward 60 percent of incident beam sunlight, and about 30 percent of the incident diffuse sunlight (of the 60 percent of diffuse light that is reflected, half will go up, and half will go down). If 20 percent of the incident sunlight is diffuse, the final fraction returned to the sky would be $80 \text{ percent} \times 0.60 \text{ wall solar retroreflectance} + 20 \text{ percent} \times [0.60 \text{ wall solar diffuse reflectance} \times (0.5 \text{ sky view factor} + 0.5 \text{ ground view factor} \times 0.10 \text{ ground albedo})] = 55 \text{ percent}$. Retroreflection can thereby reduce the solar heat gain of other urban surfaces, including ground, opposing walls, and pedestrians. However, retroreflective cool walls would provide less daylighting to neighboring buildings than would diffusely reflecting cool walls.

The retroreflector simulation setup is based on C60N60, but all walls of the neighboring and central buildings become retroreflective (C60rrN60rr). The effect of retroreflection on building energy use is also estimated using TUF-IOBES by comparing C60rrN60rr to C60N60 and the same building layout described in Section 3.2. TUF-IOBES uses a view-factor based radiation model which assumes all surfaces to be Lambertian (perfectly diffuse) reflectors. While this assumption is diametrically opposed to the working principle of a retroreflector, the effects of retroreflective materials can be approximated as shown in Figure 2. The wall is assumed to be a retroreflector for the beam solar radiation, but it is assumed to be a Lambertian reflector for the diffuse sky and ground reflected radiation. Retroreflectance of beam radiation is achieved by zeroing out wall beam reflection in the radiation model as the reflected radiative energy exits the simulation domain.

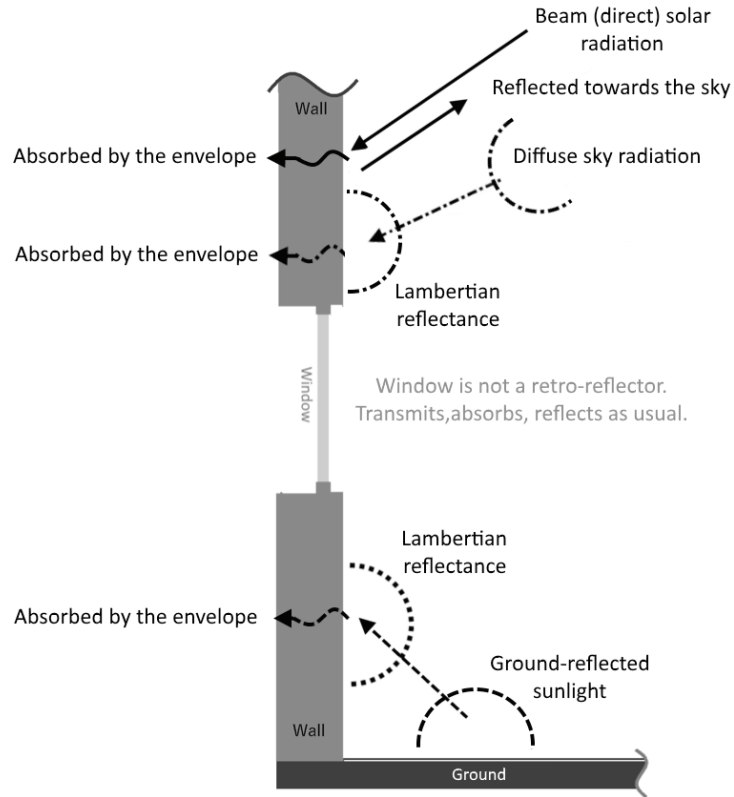


Figure 2. Sketch of TUF-IOBES radiation model for retroreflective wall simulations.

3.4 Simulation setup

3.4.1 Climate zones

Building energy use effects of cool walls are quantified in the coastal building climate zone 8 in California (California Energy Commission, 2017) represented by Fullerton in Orange County. Environmental conditions, including dry-bulb and wet-bulb air temperatures; global, beam, and diffuse solar irradiances; and wind speed are input from Typical Meteorological Year 3 (TMY3), weather data (NREL 2017). The ground albedo is set to 0.10 (asphalt concrete).

3.4.2 Other meteorological boundary conditions

In TUF-IOBES, the deep-ground temperature is set as the mean dry-bulb air temperature of the whole year from TMY3. The TMY3 air temperature and wind speed are applied at twice the building height. For wind speed, a logarithmic profile is assumed down to the building height. The wind speed at canyon half height is then estimated as $U_{\text{can}} = U_{\text{top}} \exp(-N/2)$, where U_{top} is the wind speed at the building height and N is half the canyon aspect ratio (defined as building height divided by inter-building spacing). For details see section 2.9.5 in Masson (2000). The canyon air temperature is computed from an energy balance in the urban canyon.

On outdoor surfaces, available energy (net radiation minus conduction) is converted to sensible and latent heat fluxes. Since most of the areas in California are semi-arid, a Bowen ratio of 5 is used (Taha, 1997). The Bowen ratio is the ratio of the sensible heat flux to the latent heat flux.

3.4.3 Building prototypes

Building categories. Offices are the most common type of commercial building in California comprising 1.7 percent to 21.9 percent of total building floor area depending on climate zone (Rosado, 2016). For the DOE prototype office building model (DOE, 2017), the deadband of HVAC temperature setpoints is wider at night and on weekends than during business hours (Table 1). Therefore, nighttime heating and cooling energy use is small as the building interior temperature first adjusts from the narrow deadband to the wide deadband before the HVAC systems incurs heating or cooling energy use. A large fraction of the energy use then occurs in the early morning when the building needs to be brought from the wider night-time deadband to the tighter temperature deadband for business hours. This period of morning heating and cooling is therefore coincident with cool wall effects. However, in TUF-IOBES temperature setpoints for heating and cooling cannot be varied by time of day or day of the week. Therefore TUF-IOBES is expected to overestimate nighttime HVAC energy consumption and underestimate daytime HVAC energy use. Since cool wall effects predominantly occur during the day, simulating the timing of HVAC energy accurately is critical to understanding the real impacts of cool walls on building energy use. Therefore the project team decided against simulating office buildings.

Residential buildings constitute 78 percent of the building stock in California (Rosado, 2016). In large metropolitan areas residential buildings are about evenly split between single and multi-family residences (e.g., 62 percent single-family homes versus 36 percent apartment buildings in San Diego in Table 6.7 of Rosado, 2016), while single-family residences dominate in rural areas (e.g., 94 percent single-family homes versus 4 percent apartment buildings in Lancaster in Table 6.8 of Rosado, 2016). Since the solar heat gain on neighboring walls is a function of wall-to-wall view factors (Section 2) and the wall area of the prototype multi-family residence is 4 times the wall area of the prototype single-family residence (Table A-1 of Task Report Appendix A), the multi-family residence was chosen for further study. Cool wall effects between neighboring single-family residences are expected to be smaller than the multi-family residence results in this report. Building geometrical specifications are provided in Table A-1.

Table 1. Variation with hour of week of the HVAC setpoint deadband in a DOE-supplied prototype office building model (DOE, 2017). In TUF-IOBES deadbands are constant across time of day and day of the week.

	Weekday (business hours)	Weekday (outside of business hours)	Weekend (business closed)
Day	Mon - Fri	Mon - Fri	Sat, Sun
Time (local)	07:00 – 22:00	22:00 – 07:00	00:00 – 24:00
HVAC setpoint deadband	21.0 °C to 24.0 °C	15.6 °C to 26.7 °C	15.6 °C to 26.7 °C

Adaptation of DOE residential prototype building model for use in TUF-IOBES. The multi-family residence prototype was based on a template from the U.S. Department of Energy (DOE, 2017) that was modified to follow California’s Title 24 building energy efficiency standards as described in the Task 2.1 report: *Simulated HVAC energy savings in an isolated building*. Since TUF-IOBES can only simulate simple building geometries, the original U.S. DOE building prototype as simulated in EnergyPlus in the Task 2.1 report were modified as follows.

1. In TUF-IOBES, buildings must have square footprints. Therefore, the footprint is simplified as a square that is dimensioned to match the total footprint area in EnergyPlus. The footprint area in TUF-IOBES and EnergyPlus differs by 2 percent because the TUF-IOBES wall and ground surfaces are discretized into square, equal-sized sub-areas (patches). Computational costs dictate a small number of patches; typically width and height of each building face is subdivided into two to five patches.
2. In EnergyPlus, the multi-family residence roof is pitched and the pitched roof rise (roof peak height - roof base height) is 4.1 m. TUF-IOBES can only simulate flat roofs. The height of the flat roof in TUF-IOBES was set equal to the roof base height in EnergyPlus.
3. Any façade patch has to be either a wall or a window. Therefore only discrete values of window-to-wall ratio (WWR; ratio of window area to gross wall area) can be chosen in TUF-IOBES. The WWR is 29 percent in TUF-IOBES and 28 percent in EnergyPlus.
4. In TUF-IOBES all building facades must be of identical geometry. Therefore the window size, number, and location cannot be varied by aspect. A single window near the center of each façade is assumed.
5. Exterior sunshades and interior blinds are not modeled in TUF-IOBES. All window-transmitted solar irradiance is absorbed inside the building.

6. Intermediate floors and internal mass are not considered in TUF-IOBES. That is, the buildings are empty and do not store heat in the interior space. For comparison to EnergyPlus some of the thermal loads are still reported by floor area, where floor area is the product of TUF-IOBES building footprint and EnergyPlus number of floors.

EnergyPlus and TUF-IOBES building prototype geometry, including footprint, height, length, width, window area, gross wall area, and canyon width, are compared in Table A-2.

Building vintages. The Task 2.1 report: *Simulated HVAC energy savings in an isolated building* simulates three building vintages—pre-1978, 1988, and 2016. In this report only pre-1978 buildings are simulated. As stricter building energy efficiency standards were first introduced around 1980, pre-1978 buildings have little insulation, while 1988 and 2016 buildings follow progressively stricter building energy efficiency standards with more insulation. Effects of cool walls on thermal loads of neighboring buildings are expected to be largest for the pre-1978 buildings.

Construction. Floor construction is a layer of plywood over a concrete slab over a layer of crushed rock (Yaghoobian and Kleissl, 2012). Roof, wall, building floor, and street construction are detailed in Table A-3; material properties are summarized in Table A-4 and Table A-5. Double-pane windows are chosen from the International Glazing Database (IGDB) in the Berkeley Lab WINDOW (2017) software to match EnergyPlus prototypes of overall solar heat gain coefficient (SHGC) and thermal transmittance. Angular and diffuse SHGC, absorptance, and transmittance of window glasses also derived from Berkeley Lab WINDOW are shown in Table A-6.

Equipment and people settings. Internal loads including lighting, equipment, and occupants play an important role in building energy use. The technical parameters are based on the simulations of the DOE prototype building using the DOE EnergyPlus building energy simulation model detailed in Rosado et al. (2017). Specifically, the lighting, equipment, and infiltration schedules are based on the EnergyPlus output files and the occupancy schedule is based on the EnergyPlus input files. Figure A-1 shows the TUF-IOBES inputs for lighting, equipment, occupancy, and infiltration schedules per footprint area of the multi-family residence, respectively. The conversion of lighting, equipment, and occupancy loads to conduction, convection, and radiation heat flows is shown in Table A-7. Specifications for people, equipment, and lighting follow the same scheme. First the total emitted power is split into latent and sensible fractions. Then the sensible fraction is further split into longwave, convective, and shortwave (only for lighting) fractions. People power is computed from the occupancy in Figure A-1 multiplied by the activity level in Table A-7.

HVAC is simulated simplistically in TUF-IOBES assuming (i) continuous HVAC operation with fixed temperature setpoints of 22.2 °C and 23.9 °C; (ii) constant coefficient of performance (COP = 2.64); and (iii) unlimited HVAC capacity. Therefore the heat transfer to/from the HVAC system always satisfies the air heat balance to keep the room temperature between the minimum and maximum setpoints. The constant TUF-IOBES setpoints are obtained by averaging the hourly EnergyPlus HVAC schedules over the year (Table A-7). Dividing TUF-IOBES cooling load by COP yields the cooling site energy use.

3.5 Limitations

The magnitude of cool wall effects on neighboring buildings was only analyzed for one particular building configuration. Cool wall effects are expected to be a function of the window solar heat gain coefficient, wall insulation, inter-building spacing, and window-to-wall ratio. Pre-1978 buildings with a window-to-wall ratio of 29 percent were simulated. For newer buildings with reduced window solar heat gain coefficient and improved wall insulation the cool wall effects on thermal loads of the central buildings would be smaller.

Inter-building spacing modifies the view factor from the neighboring cool wall to the central building wall. The view factor effect is difficult to test in simulations since changes to the inter-building spacing also change the view factor from ground to wall. Theory (Section 2) suggests that the increase in wall solar heat gain of the central building is proportional to the modified wall area of the neighboring buildings (A_n), the view factor to the central building wall from the extended surface comprised of all parallel neighboring walls (F_n), the increase in the albedo of the neighboring wall, and one minus the albedo of the central wall. Since view factors between two surfaces are proportional to the square of their distance, the cool wall effects reported here can be scaled to estimate gains for different inter-building spacings. However, note that F_n does not decrease with inter-building distance squared as it describes the joint view factor to the central wall from an extended surface comprised of several surfaces.

Window-to-wall ratios have different effects depending on the building where they are applied. On the neighboring building, larger window-to-wall ratios reduce the cool wall area and linearly decrease the sunlight reflected onto the central building wall. On the central building, larger window-to-wall ratios increase the solar heat gain through windows and increase cool wall effects. The window solar heat gain coefficient for diffuse sunlight is 0.52 (Table A-6), indicating that 52 percent of the solar radiation reflected from neighboring cool walls towards a window on the central building reaches the conditioned space. While conventional walls absorb 75 percent of the solar radiation reflected from neighboring cool walls, the majority of the absorbed heat is removed to the canopy air as sensible heat flux. Only a small fraction is conducted through the wall

and reaches the conditioned spaces. Therefore central-building windows increase the effects of neighboring cool walls.

A caveat to this analysis is that the daylighting effects of cool walls were ignored. However, most likely this will not impact the conclusions since residential lighting loads during daytime are small (see Figure A-1). The effect of daylighting energy savings may be significant for office buildings with large window-to-wall ratios, but office buildings are not studied in this report.

4 Results and discussion

4.1 Comparison between TUF-IOBES and EnergyPlus results

While this report focuses on *changes* in thermal loads with changing wall albedo, a brief comparison of absolute thermal loads in this report to the Task 2.1 report: *Simulated HVAC energy savings in an isolated building* is presented in this section. As described in Section 3 perfect agreement is not expected, because (i) the simulated multi-family building is different (see also Table A-2); and (ii) simplifying assumptions had to be made to run the TUF-IOBES building energy simulator compared to the more realistic building operation in EnergyPlus.

The C25N25 and C60N25 cases in TUF-IOBES are similar to the cases in EnergyPlus where a single building with all conventional and all cool walls is simulated, respectively. While neighboring buildings are not represented in EnergyPlus, a fixed reflectance of the surrounding pavements and buildings is assumed to obtain ground-reflected diffuse solar irradiance onto walls.

Table 2 shows agreement within 38 percent for cooling loads, but heating loads differ by a factor of about 5. The reasons for the differences are not well understood at present.

Relative changes in the magnitude of cooling loads are larger in EnergyPlus (-14.1 percent) than TUF-IOBES (-5.0 percent). Relative changes in heating loads are similar in EnergyPlus (10.0 percent) and TUF-IOBES (13.6 percent). The consistency in the direction and order of magnitude of the trends is encouraging, but the underestimation of cooling load savings in Table 2 suggests that TUF-IOBES cooling load savings reported for different scenarios in the following sections may be biased low.

Table 2. Annual thermal loads for the pre-1978 multi-family residence in CZ8 (Fullerton) from TUF-IOBES (this report) and EnergyPlus (Task 2.1 report: *Simulated HVAC energy savings in an isolated building*).

	Annual heating load [MWh]		Annual cooling load [MWh]	
	TUF-IOBES	EnergyPlus	TUF-IOBES	EnergyPlus
C25N25	28.7	4.6	101.3	81.2
C60N25	32.6	5.1	96.2	69.8
(a) C60N25 – C25N25	+3.9 MWh (+13.6 %)	+0.5 MWh (+10.0%)	-5.0 MWh (-5.0 %)	-11.4 MWh -14.1 %

4.2 Building-to-building interaction effect

Figure 3 (left column, i) shows that daytime heating loads are near zero for all scenarios and changing wall albedo therefore does not modify the daytime heating load. Heating load at night increases, however, when the central wall albedo is raised (C60N25 – C25N25 and C60N60 – C25N25). During the day conventional walls store more heat than cool walls. The stored heat provides a heat flux into the conditioned space and reduces heating load by up to 1 kW.

Figure 3 (right column, ii) shows that nighttime cooling loads are small and changing wall albedo therefore mostly influences the daytime cooling load. Raising the neighboring wall albedo increases cooling load of the central building due to increased solar radiation reflected from the neighboring buildings towards the central building (C25N60 – C25N25). Raising the central wall albedo reduces cooling loads due to a decrease in absorbed solar radiation (C60N25 – C25N25 and C60N60 – C25N25); the decrease in cooling loads also persists into the night due to reduced wall heat storage.

Examining the scenarios (a – d) described in Section 3.2 one by one reveals the following changes in annual thermal loads (Figure 3; Table 3):

- a) **Raising the albedo of all central walls while leaving all neighboring walls conventional (C60N25 – C25N25)** decreases annual cooling load by 5.0 MWh (5.0 percent), while annual heating load increases by 3.6 MWh (13.9 percent). Raising wall albedo of a building reduces its absorption of sunlight which reduces cooling loads and increases heating loads.
- b) **Raising the albedo of all neighboring walls when all central walls remain conventional (C25N60 – C25N25)** increases annual cooling load by 1.5 MWh (1.5 percent). The annual heating load reductions (0.1 MWh, or 0.3 percent) are negligible. These changes are small (less than 1.5 percent) compared with the

total annual heating and cooling loads of 28.7 MWh and 101.3 MWh, respectively. The negligible effect of cool walls on heating loads is likely an artifact of the way that TUF-IOBES predicts essentially zero daytime heating load. In scenario (a) the central wall heat gain is reduced by $(0.75 - 0.40)/0.75 = 47$ percent. The reduced heat storage in the walls of the central building then increases nighttime cooling loads. In scenario (b) the fractional increase in solar heat gain on the central building is only 4.3 percent (see below), which is too small to significantly influence heat storage and nighttime heating loads.

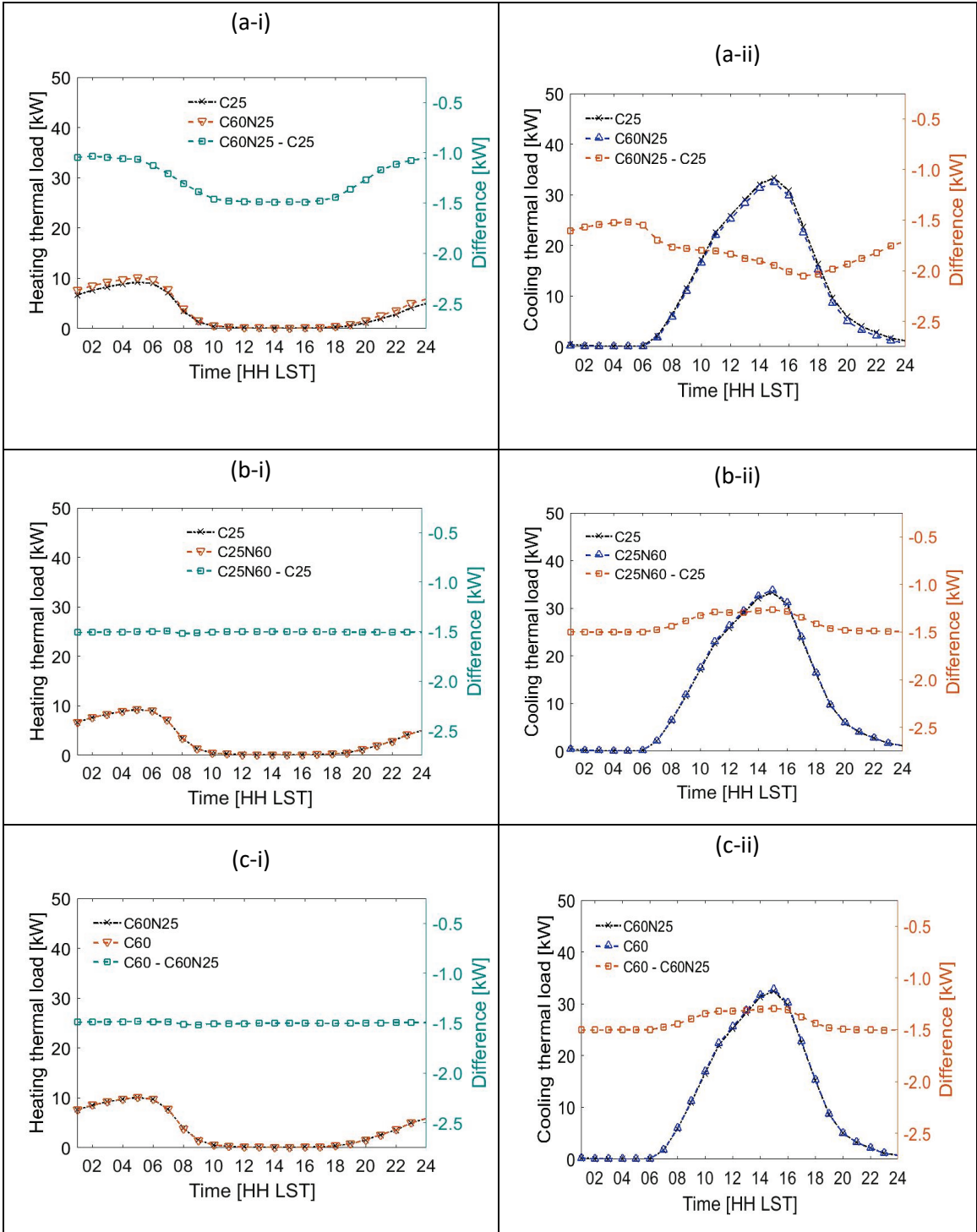
The annual cooling load increases can be compared to the fractional increase in solar heat gain predicted by Eq. (7). With $F_0 = 0.127$, $\Delta\rho_n = 0.35$, and $\rho_n = 0.25$, f_{K_0} is 4.3 percent. The fractional cooling load increase is less than the fractional solar heat gain increase, because (i) not all increase in solar heat gain incurs a cooling load, as for example on cold winter days; and (ii) cooling load depends on multiple heat transfer processes, including wall conduction (dependent on wall solar heat gain), window transmission (dependent on wall irradiance, but not on wall solar absorption), infiltration (independent of wall solar heat gain), and occupant and equipment loads (also independent of wall solar heat gain).

We can also compare the absolute increase in central building total wall solar heat gain K_0 on raising the albedo of neighboring walls to the absolute *decrease* in K_0 upon raising the albedo of the central building walls. This ratio is defined as g in Eq. (9). For the parameters in the simulations, $g = 0.09$, while the cooling load change ratio $-(C25N60 - C25N25)/(C60N25 - C25N25) = 0.30$. The cooling load change ratio is not expected to match the solar heat gain change ratio, but may allow scaling the simulation results obtained here to other building geometries and/or cool wall albedos.

- c) **Raising the albedo of all neighboring walls when all central walls are cool (C60N60 – C60N25)** increases annual cooling load by 1.2 MWh (1.2 percent). Scenario (c) is similar to scenario (b), but the effect of neighboring cool walls on annual cooling load is diminished by the high albedo of the central building walls. That is, 60 percent, rather than 25 percent, of the additional sunlight that is reflected towards the central building is reflected away from the central building, reducing the increase in annual cooling load to 1.2 MWh (1.2 percent) from 1.5 MWh (1.5 percent).
- d) **Raising the albedo of all central walls and all neighboring walls (C60N60 – C25N25)** is similar to scenario (a). But since the neighboring walls' albedos are also increased, cool walls on the central building are less effective than in case (a). The neighboring walls reflect more sunlight towards the central building. The cool walls on the central building reflect 60 percent of that sunlight, but 40 percent is absorbed. Annual cooling load in scenario (d) decreases only by 3.8

MWh (3.8 percent) versus 5.0 MWh (5.0 percent) for scenario (a). Annual heating load in scenario (d) increases by 3.9 MWh (13.7 percent), which is almost identical to scenario (a). The lack of heating load differences between scenarios (a) and (d) is consistent with scenario (b)—that is, raising the albedo of neighboring walls does not influence heating loads.

When thermal loads are only averaged over winter and summer (Figure 4), the effects of wall modifications on thermal loads are enhanced, because these limited datasets contain more days when heating and cooling are required, respectively. The wall modifications then influence the thermal loads on a larger fraction of days compared to when the entire year is considered (Figure 3).



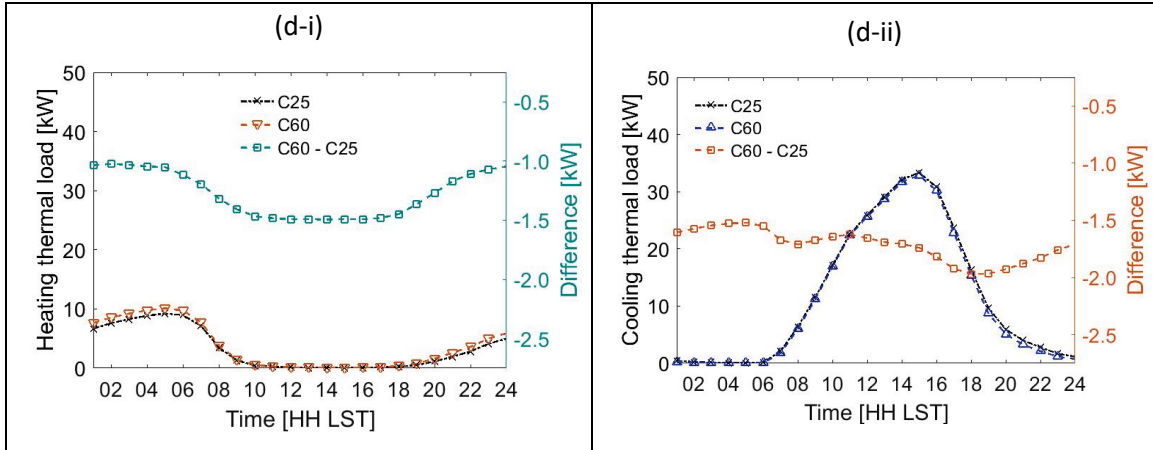
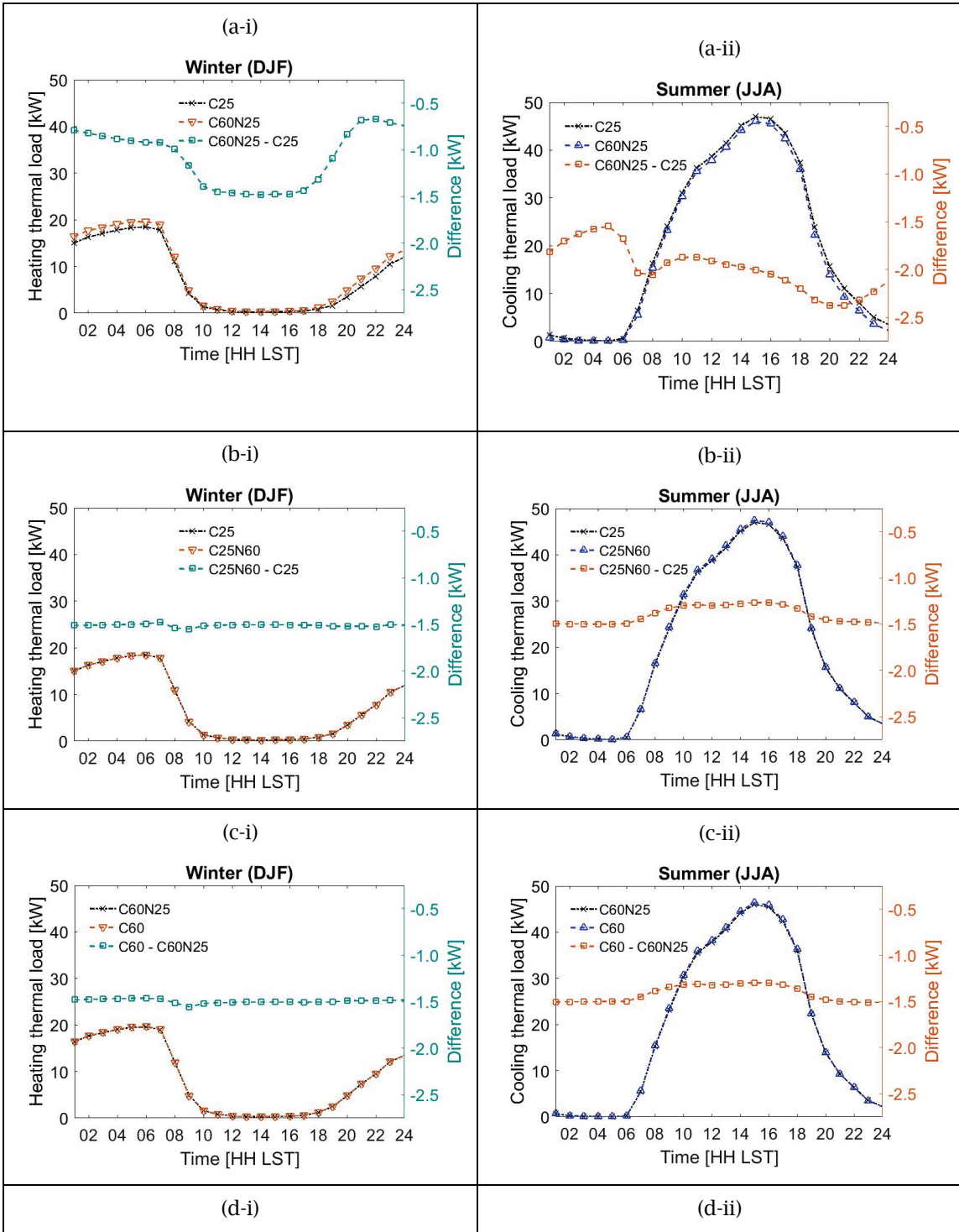


Figure 3. Average diurnal cycles of heating load (column i, left) and cooling load (column ii, right) for the central building—a pre-1978 multi-family residence in CZ8 (Fullerton)—surrounded by buildings with the same or different wall albedo. Shown are results for (a) raising the albedo of all central walls, leaving all neighboring walls conventional (C60N25 – C25N25); (b) raising the albedo of all neighboring walls when all central walls remain conventional (C25N60 – C25N25); (c) raising the albedo of the neighboring walls when all central walls are cool (C60N60 – C60N25); and (d) raising the albedo of all central walls and all neighboring walls (C60N60 – C25N25).

Table 3. Annual thermal loads for the pre-1978 multi-family residence in CZ8. The top group of four rows shows the annual results for homogeneous simulations with all-cool (C60N60) or all-conventional (C25N25) walls and combinations of cool and conventional walls. The second group of four rows shows differences in thermal loads in MWh and percent in the same order as in Figure 3.

	Annual heating load [MWh]	Annual cooling load [MWh]
C25N25	28.7	101.3
C60N60	32.7	97.5
C25N60	28.7	102.7
C60N25	32.6	96.2
(a) C60N25 – C25N25	+3.9 MWh (+13.6 %)	-5.0 MWh (+5.0 %)
(b) C25N60 – C25N25	-0.1 MWh (-0.3 %)	+1.5 MWh (+1.5 %)
(c) C60N60 – C60N25	-0.0 MWh (-0.0 %)	+1.2 MWh (+1.3 %)
(d) C60N60 – C25N25	+3.9 MWh (+13.7 %)	-3.8 MWh (+3.8 %)



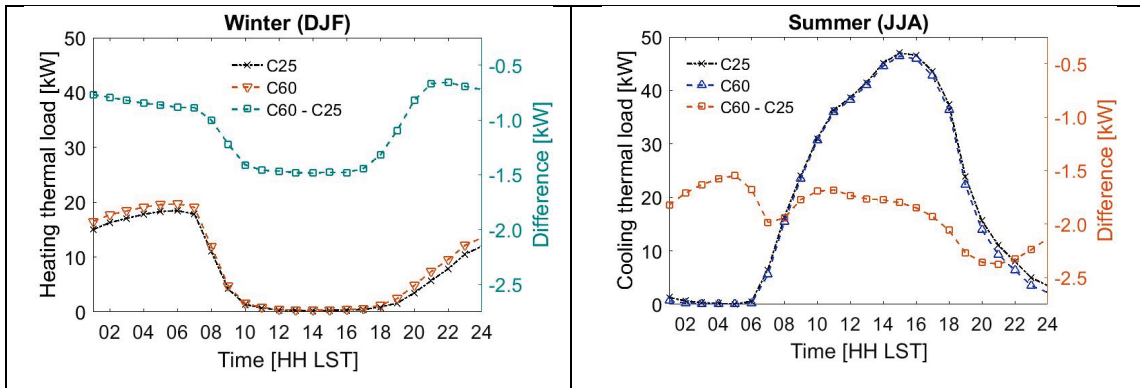


Figure 4. Seasonal analogs of Figure 3 for summer (June to August) and winter (December to February).

4.3 Retroreflective versus Lambertian Walls

For the pre-1978 multi-family residence in Fullerton retroreflective walls on all (neighboring and central) building walls (C60rrN60rr) increase heating load and decrease cooling load with respect to the C60N60 case of Lambertian cool walls on all building walls (Figure 5). Retroreflective walls completely remove the reflected beam component while Lambertian cool walls partially reflect it towards other urban surfaces. The net effect of changing to a retroreflective wall from a Lambertian wall is a reduction in average solar radiation incident on walls, which decreases cooling loads and increases heating loads.

The effect on cooling loads is largest during the day, while the effect on heating loads is largest shortly after sunrise. Shortly after sunrise, Lambertian cool walls reflect more solar radiation to surroundings walls and windows; this passive heating reduces the need for electric heating to maintain temperature setpoints. These effects are more expressed when only heating loads in winter and cooling loads in summer are considered (Figure 6).

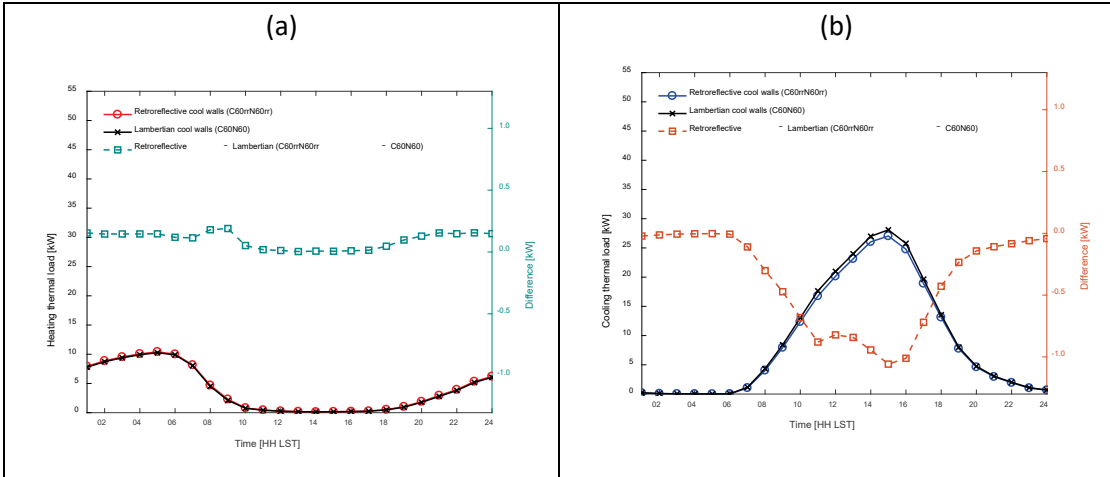


Figure 5. Comparison of the average diurnal cycle of heating (left, a) and cooling (right, b) loads for buildings with Lambertian reflector walls with wall albedo of 0.60 (C60N60) and walls with retroreflectors with wall albedo of 0.60 (C60rrN60rr). Results are averaged over the year for the pre-1978 multi-family residence in CZ8 (Fullerton).

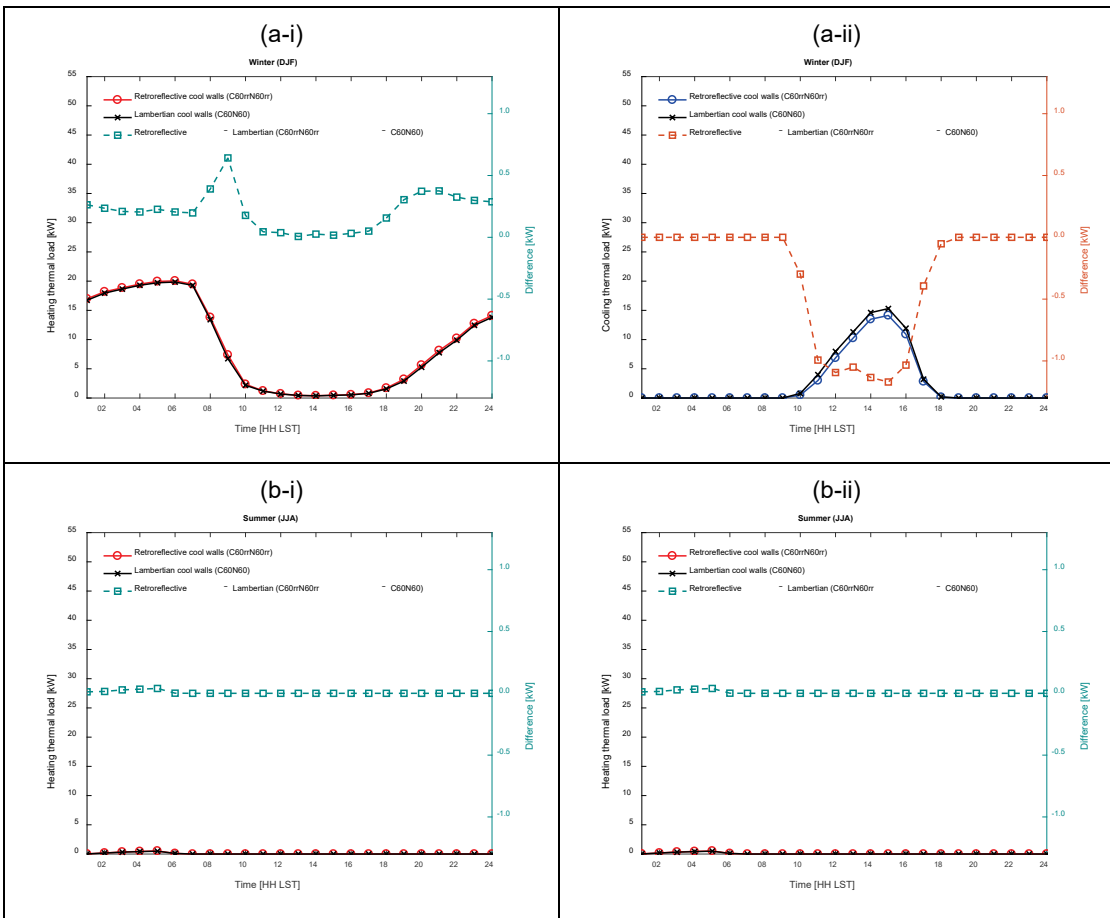


Figure 6. Seasonal analogs of Figure 5 for winter (December to February, a) and summer (June to August, b).

Table 4 shows the thermal loads for buildings with retroreflective walls and the change with respect to a multi-family residence with Lambertian cool walls. Retroreflective walls (C60rrN60rr) decrease annual cooling energy use by 3.3 MWh (4.0 percent) with respect to buildings with Lambertian cool walls (C60N60). The cooling benefit comes at the expense of a 0.9 MWh (2.6 percent) increase in annual heating load.

Table 4. Seasonal and annual heating and cooling loads for pre-1978 multi-family residence in CZ8 with Lambertian cool walls (C60N60) and retroreflective walls (C60rrN60rr). The retroreflective wall results are reported as load with retroreflective walls of albedo 0.60 minus the load with Lambertian walls of albedo 0.60.

	Heating load			Cooling load		
	Lambertian cool walls (C60N60)	Change due to retroreflective walls (C60rrN60rr – C60N60)		Lambertian cool walls (C60N60)	Change due to retroreflective walls (C60rrN60rr – C60N60)	
	[MWh]	[MWh]	[%]	[MWh]	[MWh]	[%]
Winter (DJF)	19.1	+0.5	+2.6	6.2	-0.7	-11.3
Summer (JJA)	0.1	+0.0	+9.4	37.9	-1.0	-2.6
Year	34.3	+0.9	+2.6	81.6	-3.3	-4.0

5 Conclusions

This report investigates the effects of reflective (cool) walls on building thermal loads for multi-family residences in California. The annual cooling load decreases but the annual heating load increases with increasing wall albedo. More detailed results on cool wall effects on the building where the cool wall is applied can be found in the Task 2.1 report: *Simulated HVAC energy savings in an isolated building*.

The unique analysis in this report is the interaction effect between buildings with and without cool walls. For this discussion the neighboring building is the building where the cool wall is applied, while the central building receives the sunlight reflected by the neighboring cool wall. Raising the albedo of neighboring walls reflects more sunlight onto the central building, which can increase its cooling load and reduce its heating load. Central building thermal loads and the outdoor thermal environment were simulated for a 5 × 5 array of multi-family residences separated by 23.3 m in California climate zone 8 (Fullerton).

In the first analysis set, all walls were assumed to be perfectly diffuse (Lambertian) reflectors. When the central building has conventional walls (albedo 0.25), raising the albedo of all neighboring walls to 0.60 (cool) from 0.25 (conventional) increases the central building's cooling load by 1.5 MWh (1.5 percent); the central building's heating

load is unaffected. If the central building also has cool walls (albedo 0.60), the central building's cooling load only increased by 1.2 MWh (1.3 percent). The negligible effect of cool walls on heating loads is likely an artifact of the way that TUF-IOBES predicts essentially zero daytime heating load. The cooling load increase for the central building upon raising the albedo of all neighboring walls are smaller than the cooling load decreases for the central building upon raising the albedo of its own walls (5.0 MWh, or 5.0 percent). Considering interactions between buildings therefore does not change the direction of the cool wall effects on all buildings combined. The equations derived in the theory section may allow scaling the simulation results obtained here to other building geometries and/or cool wall albedos.

In the second analysis set, all walls are assumed to retroreflected beam (direct) sunlight. Retroreflectors further enhance the cool wall effects, because retroreflective walls completely remove the reflected beam component while Lambertian cool walls partially reflect it towards other urban surfaces. Retroreflector effects were simulated in homogeneous arrays of buildings where all wall albedos are 0.60, but all walls are either retroreflective or Lambertian reflectors. Retroreflective walls decrease annual cooling loads by 3.3 MWh (4.0 percent) with respect to buildings with Lambertian cool walls. However, the cooling benefit comes at the expense of a 0.9 MWh (2.6 percent) increase in annual heating load.

6 References

- Akbari H, Levinson R. 2008. Evolution of cool roof standards in the United States. *Advances in Building Energy Research* 2, 1-32, <http://doi.org/10.3763/aber.2008.0201>
- American Society of Heating, Refrigerating and Air-conditioning Engineers Inc. ANSI/ASHRAE/IESNA Standard 90.1-2004.
- Berkeley Lab WINDOW v.7.4.8.0. 2017. <https://windows.lbl.gov/software/window/window.html>, accessed May 15, 2017
- Building in California, California Climate Zone, <http://buildingincalifornia.com/california-climate-zones/>, Accessed July 11, 2017.
- California Energy Commission. 2017. California Energy Maps. http://www.energy.ca.gov/maps/renewable/building_climate_zones.html. Accessed May 15, 2017.
- CRRC. 2017. Cool roof rebates and codes. Cool Roof Rating Council. Retrieved 2017-08-05 from <http://coolroofs.org/resources/rebates-and-codes> .

Energy Information Administration. 2017. <https://www.eia.gov/outlooks/ieo/world.cfm>, accessed May 15, 2017.

Energy Information Administration. 2009. Household Energy Use in California, 2009, https://www.eia.gov/consumption/residential/reports/2009/state_briefs/pdf/CA.pdf, accessed May 15, 2017

Masson V. 2000. A physically-based scheme for the urban energy budget in atmospheric models. *Boundary-Layer Meteorology* 94: 357-397, <https://doi.org/10.1023/A:1002463829265>.

National Renewable Energy Laboratory. 2017. National Solar Radiation Data Base, 1991-2005 Update: Typical Meteorological Year 3. http://rredc.nrel.gov/solar/old_data/nsrdb/1991-2005/tmy3/. Accessed May 15, 2017.

Rosado PJ. 2016. Evaluating cool impervious surfaces: application to an energy-efficient residential roof and to city pavements. Ph.D. dissertation, UC Berkeley. <http://escholarship.org/uc/item/6bf80485> .

Taha H. 1997. Urban Climates and Heat Islands: Albedo, Evapotranspiration, and Anthropogenic Heat. *Energy and Buildings* 25: 99-103, [https://doi.org/10.1016/S0378-7788\(96\)00999-1](https://doi.org/10.1016/S0378-7788(96)00999-1) .

U.S. Department of Energy (2017), <https://www.energycodes.gov/development/>, accessed May 15, 2017.

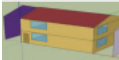
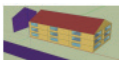
Yaghoobian N, Kleissl J. 2012. An indoor-outdoor building energy simulator to study urban modification effects on building energy use – Model description and validation. *Energy and Buildings* 54: 407-417, <https://doi.org/10.1016/j.enbuild.2012.07.019> .

Yaghoobian N, Kleissl J. 2012. Effect of reflective pavements on building energy use. *Urban Climate* 2: 25-42, <https://doi.org/10.1016/j.uclim.2012.09.002> .

Task Report Appendix A: Building Specifications

The appendix contains details of the building specifications discussed in Section 3.4.

Table A-1. Geometric parameters for each U.S. DOE building prototype as simulated in EnergyPlus in the Task 2.1 report: *Simulated HVAC energy savings in an isolated building*. TUF-IOBES parameters are shown in Table A-2.

Building type	Prototype sketches	Footprint area [m ²] ^a	Roof area [m ²]	Building height [m]	Building length × width [m]	Floors ^b	Whole-building window to wall ratio [%] ^c	Whole-building gross wall area [m ²]	Whole-building window area [m ²]
Single-family residence		112	118	5.2	12.2 × 9.2	2	14	235	33
Multi-family residence		725	785	7.8	36.5 × 19.8	3	26	958	246

^a Since in TUF-IOBES only buildings with square footprints can be simulated, footprint area is taken as the similarity parameter and building length is taken as the square root of the footprint area.

^b The number of floors refers to the EnergyPlus setup, while in TUF-IOBES the building is simulated as an empty shell.

^c Window-to-wall ratio is defined as the ratio of window area to gross wall area.

Table A-2. Comparison of the building geometrical properties between the EnergyPlus (E+) simulations in the Task 2.1 report: *Simulated HVAC energy savings in an isolated building* and TUF-IOBES. Only single-family and multi-family residences are considered in this chapter.

Building type	Footprint area [m ²]		Height H [m]		Length × width [m × m]		Whole-building gross wall area [m ²]		Whole-building window area [m ²]		Window-to-wall ratio ^a [%]		Canyon width W_c ^b [m]	Canyon aspect ratio H / W_c ^b [-]
	E+	TUF-IOBES	E+	TUF-IOBES	E+	TUF-IOBES	E+	TUF-IOBES	E+	TUF-IOBES	E+	TUF-IOBES	TUF-IOBES	TUF-IOBES
Multi-family residence	723	740	7.8	7.8	36.5 × 19.8	27.2 × 27.2	878	849	246	242	28	29	23.3	0.33

^a Window-to-wall ratio is defined as the ratio of window area to gross wall area.

^b Canyon width and canyon aspect ratio are not shown for EnergyPlus since EnergyPlus simulates an isolated building.

Table A-3. Roof, walls, building floor, and street construction. ^a

Surface	Layer	Multi-family residence
Roof	Top	Asphalt shingle
	2	OSB_ 1/2 in
	3	Roof insulation ^b
	4	½ in drywall
Walls	Outside	25 mm stucco
	2	200 mm normal weight concrete wall
	3	Wall insulation ^b
	4	13 mm gypsum board
Floor	Top	Plywood
	2	Concrete
	3	Crushed rock
Street	Top	Asphalt concrete
	2	Crushed rock

^a The thermal and roughness material properties are defined in Table A-4 and Table A-5.

^b The thickness of walls and roof insulation varies by building vintage and climate zone.

Table A-4. Material properties.

Materials	Thickness [m]	Conductivity [W/m · K]	Density [kg/m ³]	Specific heat [kJ/kg · K]	Thermal resistance [m ² · K/W]	Thermal emittance [-]	Solar absorptance [-] ^b	Texture
Metal surface	0.001	45.28	7,824	0.50	0.000018	0.90	0.70	Smooth
25 mm stucco	0.025	0.72	1,856	0.84	0.035	0.90	0.75	Smooth
200 mm normal weight concrete wall	0.203	2.31	2,322	0.83	0.088	0.90	0.70	Medium rough
13mm gypsum board	0.013	0.16	800	1.09	0.079	0.90	0.70	Smooth
Wall insulation ^a	Table A-5	0.06	43	1.21	Table A-5	0.90	0.70	Medium rough
Asphalt shingle	0.006	0.08	1,121	1.26	0.077	0.90	0.80	Medium rough
OSB_1/2 in	0.013	0.12	545	1.21	0.109	0.90	0.70	Medium smooth
Roof insulation ^a	Table A-5	0.06	42	0.78	Table A-5	0.90	0.70	Rough
Drywall_1/2 in	0.013	0.16	801	1.09	0.079	0.90	0.70	Medium smooth
Asphalt	0.070	0.75	2,110	0.92	0.093	0.95	0.82	Very rough
Concrete	0.070	1.51	2,400	0.88	0.046	0.95	0.82	Very rough
Plywood	0.019	0.12	545	1.22	0.158	0.90	0.80	Medium smooth
Crushed rock	0.200	0.95	1,200	1.05	0.211	0.90	0.65	Medium smooth

^a Wall and roof insulation properties depend on the climate zone and are provided in Table A-5.

^b If the material is opaque to sunlight, solar absorptance = 1 – solar reflectance.

Table A-5. Wall and roof insulation thickness and thermal resistance for the pre-1978 multi-family residences in CZ8. ^a

Vintage	Pre-1978
Wall insulation thickness [m]	0.05
Wall insulation thermal resistance [m ² ·K/W]	0.82
Roof insulation thickness [m]	0.15
Roof insulation thermal resistance [m ² ·K/W]	2.51

^a For insulation materials, $L = R \times k$, where L = thickness [m], R = thermal resistance [m²·K/W], and k = thermal conductivity [W/m·K].

Table A-6. Angular solar heat gain coefficient (SHGC), visible transmittance, and visible absorptance of window glass for pre-1978 buildings ^{a,b}.

Incident angle (°)	SHGC	Transmittance	Absorptance (first pane)	Absorptance (second pane)
0	0.611	0.346	0.053	0.513
10	0.609	0.348	0.053	0.511
20	0.605	0.353	0.053	0.506
30	0.597	0.362	0.054	0.496
40	0.583	0.373	0.055	0.478
50	0.555	0.388	0.055	0.477
60	0.500	0.403	0.053	0.390
70	0.393	0.411	0.046	0.386
80	0.123	0.370	0.031	0.123
90	0.611	0.346	0.053	0.513
Diffuse	0.522	0.420	0.375	0.051

^a Window properties are simulated by the Berkeley Lab WINDOW v.7.4.8.0 (2017) software.

^b Window is opaque to thermal infrared radiation. Thermal transmittance $U = 1/(R_{in} + R_{window} + R_{out}) = 3.65$ W/(m²·K) for the pre-1978 building, where R_{in} , R_{window} , and R_{out} are the thermal resistances of the inside air film, window, and outside air film, respectively.

Table A-7. Lighting splits, equipment splits, and occupancy splits from the U.S. DOE building prototypes as simulated in this report and the Task 2.1 report: *Simulated HVAC energy savings in an isolated building.*

Splits		Multi-family residence	
People splits	Activity Level [W / person]	134	
	Latent fraction	0.38	
	Sensible fraction	0.62	
	split into:		
	LW radiant fraction	0.00	
	Convective fraction	1.00	
Equipment splits	Latent fraction	0.12	
	Sensible fraction	0.88	
	split into:		
		LW radiant fraction	0.48
	Convective fraction	0.52	
Lighting splits	Sensible fraction	1.00	
	split into:		
		SW radiant fraction	0.20
		LW radiant fraction	0.60
		Convective fraction	0.20
	Fraction of heat return air duct	0.00	

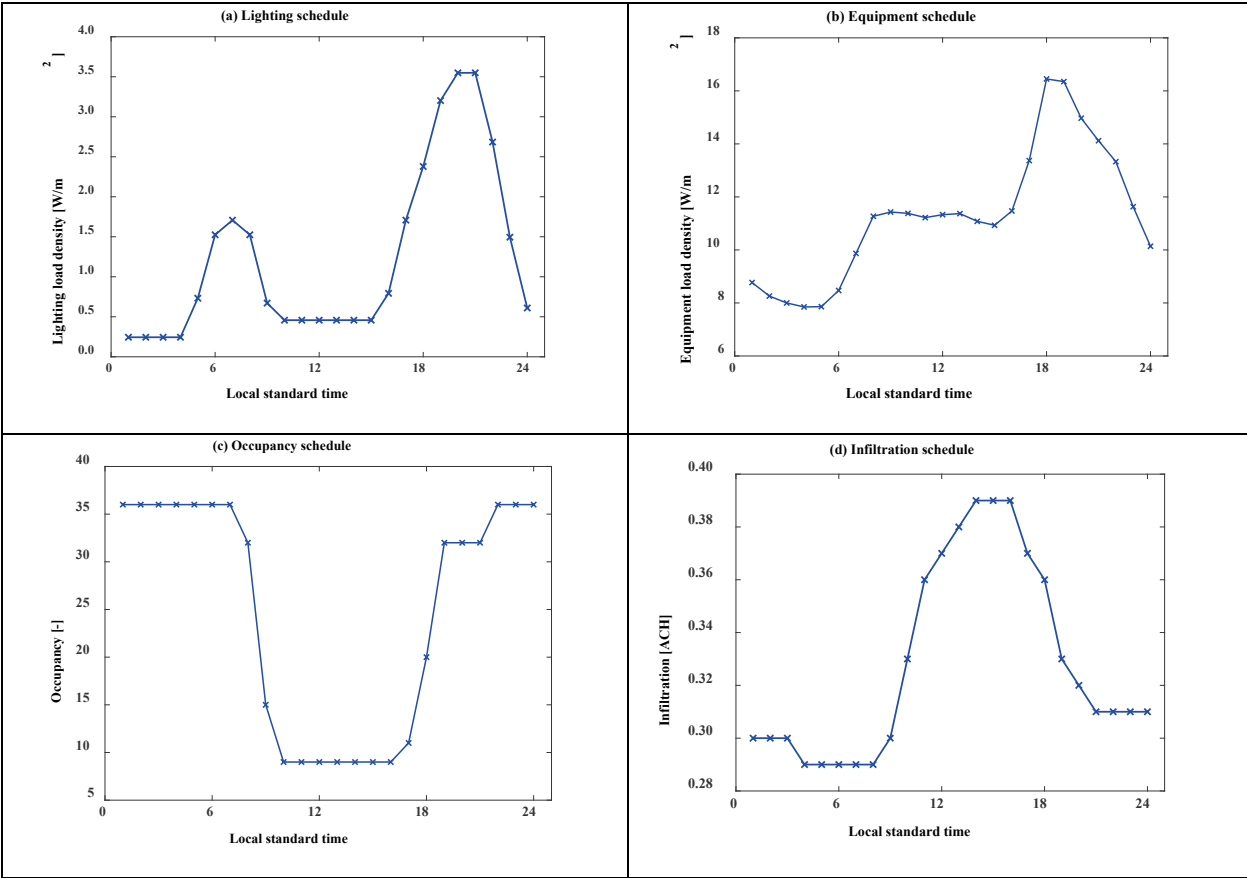


Figure A-1. Lighting load density, equipment load density, occupancy, and infiltration schedules for the multi-family residence in EnergyPlus and TUF-IOBES. Lighting and equipment load densities shown here were calculated by normalizing whole-building loads to TUF-IOBES building footprint area.